Korean J. Chem. Eng., **27**(1), 340-354 (2010)
DOI: 10.1007/s11814-009-0309-1

A new approach for optimization of electrospun nanofiber formation process

Mohammad Ziabari, Vahid Mottaghitalab, and Akbar Khodaparast Haghi†

University of Guilan, P.O. Box 3756, Rasht, Iran
(*Received 5 March 2009 • accepted 21 June 2009*)

Abstract−Precise control of fiber diameter during electrospinning is very crucial for many applications. A systematic and quantitative study on the effects of processing variables enables us to control the properties of electrospun nanofibers. In this contribution, response surface methodology (RSM) was employed to quantitatively investigate the simultaneous effects of four of the most important parameters, namely solution concentration (C), spinning distance (d), applied voltage (V) and volume flow rate (Q), on mean fiber diameter (MFD) as well as standard deviation of fiber diameter (StdFD) in electrospinning of polyvinyl alcohol (PVA) nanofibers.

Key words: Electrospinning, Nanofibers, Fiber Diameter, Processing Variables, Response Surface Methodology

INTRODUCTION

Electrospinning is a novel and efficient method by which fibers with diameters in nanometer scale, termed nanofibers, can be achieved. In electrospinning, a strong electric field is applied on a droplet of polymer solution (or melt) held by its surface tension at the tip of a syringe's needle (or a capillary tube). As a result, the pendent drop becomes highly electrified and the induced charges are distributed over its surface. Increasing the intensity of electric field, the surface of the liquid drop will be distorted to a conical shape known as the Taylor cone [1]. Once the electric field strength exceeds a threshold value, the repulsive electric force dominates the surface tension of the liquid and a stable jet emerges from the cone tip. The charged jet is then accelerated toward the target and rapidly thins and dries as a result of elongation and solvent evaporation. As the jet diameter decreases, the surface charge density increases and the resulting high repulsive forces split the jet to smaller jets. This phenomenon may take place several times leading to many small jets. Ultimately, solidification occurs and fibers are deposited on the surface of the collector as a randomly oriented nonwoven mat [2-5]. Fig. 1 shows a schematic illustration of electrospinning setup.

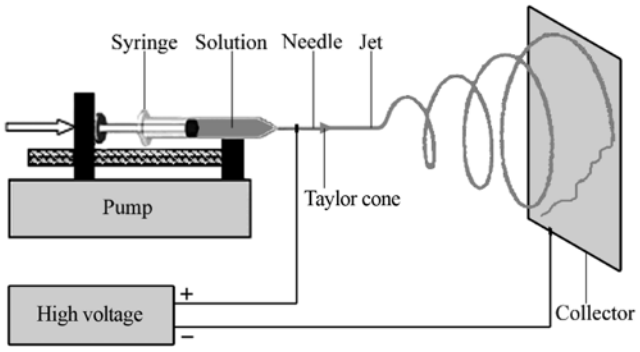

Fig. 1. A typical image of electrospinning process [6].

†To whom correspondence should be addressed.
E-mail: Haghi@Guilan.ac.ir

According to various outstanding properties such as very small fiber diameters, large surface area per mass ratio [3], high porosity along with small pore sizes [7,8], flexibility, and superior mechanical properties [9], electrospun nanofiber mats have found numerous applications in diverse areas. For example, in the biomedical field nanofibers play a substantial role in tissue engineering [10-12], drug delivery [13,14], and wound dressing [15,16]. Moreover, the use of nanofibers in protective clothing [7], filtration technology [17,18] and reinforcement of composite materials [9,19] is extremely significant for developing specific products by manipulation of materials in nanoscales. In the mean time, those applications are related to micro-electronics like battery [20], supercapacitors [21], transistors [22], sensors [23], and display devices [24].

The physical characteristics of electrospun nanofibers such as fiber diameter depend on various parameters which are mainly divided into three categories: solution properties (solution viscosity, solution concentration, polymer molecular weight, and surface tension), processing conditions (applied voltage, volume flow rate, spinning distance, and needle diameter), and ambient conditions (temperature, humidity, and atmosphere pressure) [25]. Numerous applications require nanofibers with desired properties, suggesting the importance of the process control. This end may not be achieved unless having a comprehensive outlook of the process and quantitative study of the effects of governing parameters. In addition, qualitative description of the experimental observations are not adequate to derive general conclusions, and either the equations governing behavior of the system must be found or appropriate empirical models need be presented. In Ziabicki's words, "in the language of science 'to explain' means to put forward a quantitative model which is consistent with all the known data and capable of predicting new fact" [26].

Employing a model to express the influence of electrospinning parameters will help us obtain a simple and systematic way for presenting the effects of variables, thereby enabling control of the process. Furthermore, it allows us to predict the results under a new combination of parameters. Hence, without conducting any experiments, one can easily estimate features of the product under unknown conditions. An empirical model therefore tells us to what extent the

output of a system will change if one or more parameters increased or decreased. This is very helpful and leads to a complete understanding of the process and the effects of parameters.

Despite the surge in attention to different aspects of electrospinning process, a few investigations have addressed the quantitative study of the effects of the parameters. Changing the behavior of materials in nano-scale, presence of electric field, branching of the jet, random orientation of fibers, etc. made the analysis of the process extremely complex and difficult, so that to date there has been no reliable theory capable of describing the phenomenon. Furthermore, the development of an empirical model has also been impeded due to the lack of systematic and characterized experimentations with appropriate designs. Adding to the difficulty is the number of parameters involved in the electrospinning process and the interactions between them, which has made it almost impossible to investigate the simultaneous effects of all variables.

Affecting the characteristics of the final product such as physical, mechanical and electrical properties, fiber diameter is one of the most important structural features in electrospun nanofiber mats. Podgorski et al. [27] indicated that filters composed of fibers with smaller diameters have higher filtration efficiencies. This was also proved by the work presented by Qin et al. [17]. Ding et al. [28] also reported that sensitivity of sensors increased with decreasing the mean fiber diameter due to the higher surface area. It was also shown that in polymer batteries consisting of electrospun polyvinylidene fluoride (PVdF) fibrous electrolyte, lower mean fiber diameter results in a higher electrolyte uptake thereby increasing ionic conductivity of the mat [29]. Furthermore, Moroni et al. [30] found that fiber diameters of electrospun polyethylene oxide terephthalate/polybutylene terephthalate (PEOT/PBT) scaffolds influencing cell seeding, attachment, and proliferation. They also studied the release of dye incorporated in electrospun scaffolds and observed that with increasing fiber diameter, the cumulative release of the dye (methylene blue) decreased. Carbonization and activation conditions as well as the structure and properties of the ultimate carbon fibers are also affected by the diameters of the precursor polyacrylonitril (PAN) nanofibers [31]. Consequently, precise control of the electrospun fiber diameter is very crucial.

A few techniques such as orthogonal experimental design [32] and using power law relationships [31] have been reported in the literature for quantitative study of electrospun nanofiber. However, researchers mostly paid attention to response surface methodology (RSM) technique due to its simplicity and its ability to take into account the interactions between the parameters. Sukigara et al. [33] employed RSM to model mean fiber diameter of electrospun regenerated Bombyx mori silk with electric field and concentration at two spinning distances. They applied a full factorial experimental design at three levels of each parameter, leading to nine treatments of factors, and used a quadratic polynomial to establish a relationship between mean fiber diameter and the variables. Increasing the concentration at constant electric field resulted in an increase in mean fiber diameter. Different impacts for the electric field were observed depending on solution concentration. Since the effects of solution concentration and electric field strength on mean fiber diameter changed at different spinning distances, they suggested that some interactions and coupling effects are present between the parameters.

Gu et al. [34,35] also exploited the RSM for quantitative study of polyacrylonitril (PAN) and poly D,L-lactide (PDLA), respectively. The only difference observed in the procedure was the use of four levels of concentration in the former case. They included the standard deviation of fiber diameter in their investigations by which they were able to provide additional information regarding the morphology of electrospun nanofibers and its variations at different conditions. Furthermore, they analyzed the significance of factors in the models in order to understand the level of influence of each parameter. In the case of PAN, voltage as well as its interaction with concentration had no considerable effects on both mean and standard deviation of fiber diameter. Hence, they eliminated the terms corresponding to these factors, thereby obtaining simplified quadratic models according to which mean and standard deviation of fiber diameter increased with polymer concentration. On the contrary, both voltage and its interaction with concentration were found to be significant in the case of PDLA. However, the effect of polymer concentration was more pronounced. Increasing voltage at constant concentration favored thinner fiber formation which gained momentum with increasing concentration. Fibers with more uniform diameters (less standard deviation) were obtained at higher applied voltage or concentration.

In the most recent investigation in this field, Yördem et al. [36] used RSM to correlate mean and coefficient of variation (CV) of electrospun PAN nanofibers to solution concentration and applied voltage at three different spinning distances. They employed a face-centered central composite design (FCCD) along with a full factorial design at two levels resulting in 13 treatments at each spinning distance. A cubic polynomial was then used to fit the data in each case. As in previous studies, fiber diameter was very sensitive to changes in solution concentration. Voltage effect was more significant at higher concentrations, demonstrating the interaction between parameters.

According to previous studies, there are some interactions between electrospinning parameters. However, they only investigated the simultaneous effects of two variables; therefore they were unable to thoroughly capture the interactions which exist between the parameters. For instance, Sukigara et al. [33] and Yördem et al. [36] both agreed that spinning distance has a significant influence on fiber diameter and that this effect varies when solution concentration and/or applied voltage altered. Although, their study promotes our knowledge about quantitative analysis of the electrospinning process, it still suffers from a lack of comprehensiveness. In addition, in every research where modeling of a process is targeted, the obtained models need to be evaluated with a set of test data which were not used in establishing the relationships. Otherwise, the effectiveness of the models will not be guaranteed and there will always be an uncertainty in the prediction of the models in new conditions. It could be claimed that the presented models in previous studies were not evaluated with a series of test data. Therefore, their models may not generalize well to new data and their prediction ability is obscure.

In this contribution for the first time, the simultaneous effects of four electrospinning parameters (solution concentration, spinning distance, applied voltage, and volume flow rate) on mean and standard deviation of electrospun polyvinyl alcohol (PVA) fiber diameter were systematically investigated. PVA, the largest volume synthetic water-soluble polymer produced in the world, is commercially manufactured by the hydrolysis of polyvinyl acetate. The excellent chemi-

cal resistance and physical properties of PVA along with non-toxicity and biodegradability have led to its broad industrial applications such as textile sizing, adhesive, paper coating, fibers, and polymerization stabilizers [37,38]. Several patents reported a process for production of ultrahigh tensile strength PVA fibers comparable to Kevlar® [39-41]. PVA has found many applications in biomedical uses as well, due to its biocompatibility [42]. For instance, PVA hydrogels were used in regenerating articular cartilages [43,44], artificial pancreas [45], and drug delivery systems [46,47]. More recently, PVA nanofibers were electrospun and used as a protein delivery system [48], retardation of enzyme release [48] and wound dressing [49]. The objective of this paper is to use RSM to establish quantitative relationships between electrospinning parameters and mean and standard deviation of fiber diameter as well as to evaluate the effectiveness of the empirical models with a set of test data.

EXPERIMENTAL

1. Solution Preparation and Electrospinning

PVA with molecular weight of 72,000 g/mol and degree of hydrolysis of >98% was obtained from Merck and used as received. Distilled water as solvent was added to a predetermined amount of PVA powder to obtain 20 ml of solution with desired concentration. The solution was prepared at 80 ºC and gently stirred for 30 min to expedite the dissolution. After the PVA had completely dissolved, the solution was transferred to a 5 ml syringe and became ready for spinning of nanofibers. The experiments were carried out on a horizontal electrospinning setup shown schematically in Fig. 1. The syringe containing PVA solution was placed on a syringe pump (New Era NE-100) used to dispense the solution at a controlled rate. A high voltage DC power supply (Gamma High Voltage ES-30) was used to generate the electric field needed for electrospinning. The positive electrode of the high voltage supply was attached to the syringe needle via an alligator clip and the grounding electrode was connected to a flat collector wrapped with aluminum foil where electrospun nanofibers were accumulated to form a nonwoven mat. The electrospinning was carried out at room temperature. Subsequently, the aluminum foil was removed from the collector. A small piece of mat was placed on the sample holder and gold sputter-coated (Bal-Tec). Thereafter, the micrograph of electrospun PVA fibers was obtained by scanning electron microscope (SEM, Phillips XL-30) under magnification of 10,000×. Quite recently, the authors established a couple of image analysis based techniques entitled as direct tracking [50,51] and new distance transform [52,53] for measuring electrospun nanofiber diameter. In this study, fiber diameter distribution for each specimen was determined from the SEM micrograph by new distance transform method due to its effectiveness. SEM micrographs of typical PVA electrospun nanofiber mats are shown in Fig. 5 in Appendix.

2. Choice of Parameters and Range

Variables which potentially can alter the electrospinning process are large. Hence, investigating all of them in the framework of one single research would almost be impossible. However, some of these parameters can be held constant during experimentation. For instance, performing the experiments in a controlled environmental condition, which is the concern in this study, the ambient parameters (i.e., temperature, air pressure, and humidity) are kept unchanged. Solution viscosity is affected by polymer molecular weight, solution concentration, and temperature. For a particular polymer (constant molecular weight) at a fixed temperature, solution concentration would be the only factor influencing the viscosity. In this circumstance, the effect of viscosity could be determined by the solution concentration. Therefore, there would be no need for viscosity to be considered as a separate parameter.

In this regard, solution concentration (C), spinning distance (d), applied voltage (V), and volume flow rate (Q) were selected to be the most influential parameters. The next step is to choose the ranges over which these factors are varied. Process knowledge, which is a combination of practical experience and theoretical understanding, is required to fulfill this step. The aim is here to find an appropriate range for each parameter where dry, bead-free, stable, and continuous fibers without breaking up to droplets are obtained. This goal could be achieved by conducting a set of preliminary experiments while having the previous works in mind along with utilizing the reported relationships.

The relationship between intrinsic viscosity ([η]) and molecular weight (M) is given by the well-known Mark-Houwink-Sakurada equation as follows:

$$[\eta]=KM^{a} \quad (1)$$

where K and a are constants for a particular polymer-solvent pair at a given temperature [54]. For the PVA with molecular weight in the range of 69,000 g/mol<M<690,000 g/mol in water at room temperature, K=6.51 and a=0.628 were found by Tacx et al. [55]. Using these constants in the equation, the intrinsic viscosity for PVA in this study (molecular weight of 72,000 g/mol) was calculated to be [η]=0.73.

Polymer chain entanglements in a solution can be expressed in terms of Berry number (B), which is a dimensionless parameter defined as the product of intrinsic viscosity and polymer concentration (B=[η]C) [56]. For each molecular weight, there is a lower critical concentration at which the polymer solution cannot be electrospun. Koski et al. [57] observed that B>5 is required to form stabilized fibrous structures in electrospinning of PVA. On the other hand, they reported the formation of flat fibers at B>9. Therefore, the appropriate range in this case could be found within 5<B<9 domain, which is equivalent to 6.8%<C<12.3% in terms of concentration of PVA. Koski et al. [57] observed that beaded fibers were electrospun at low solution concentration. Hence, it was thought that the domain 8%≤C≤12% would warrant the formation of stabilized bead-free fibers with circular cross-sections. This domain was later justified by some preliminary experiments.

As for determining the appropriate range of applied voltage, referring to previous works, it was observed that the changes of voltage lay between 5 kV to 25 kV depending on experimental conditions; voltages above 25 kV were rarely used. Afterwards, a series of experiments were done to obtain the desired voltage domain. At V<10 kV, the voltage was too low to spin fibers and 10 kV≤V<15 kV resulted in formation of fibers and droplets; in addition, electrospinning was impeded at high concentrations. In this regard, 15 kV≤V≤ 25 kV was selected to be the desired domain for applied voltage.

The use of 5-20 cm for spinning distance was reported in the literature. Short distances are suitable for highly evaporative solvents, whereas it results in wet coagulated fibers for nonvolatile solvents

due to insufficient evaporation time. Since water was used as solvent for PVA in this study, short spinning distances were not expected to be favorable for dry fiber formation. Afterwards, this was proved by experimental observations and 10 cm≤d≤20 cm was considered as the effective range for spinning distance.

Few researchers have addressed the effect of volume flow rate. Therefore, in this case, the attention was focused on experimental observations. At Q<0.2 ml/h, in most cases especially at high polymer concentrations, the fiber formation was hindered due to insufficient supply of solution to the tip of the syringe needle. Whereas, excessive feed of solution at Q>0.4 ml/h incurred formation of droplets along with fibers. As a result, 0.2 ml/h≤Q≤0.4 ml/h was chosen as the favorable range of flow rate in this study.

3. Experimental Design

The aim of experimental design is to provide reasonable and scientific answers to such questions. In other words, experimental design comprises sequential steps to ensure efficient data gathering process and leading to valid statistical inferences [58,59].

Consider a process in which several factors affect a response of the system. In this case, a conventional strategy of experimentation, which is extensively used in practice, is the *one-factor-at-a-time* approach. The major disadvantage of this approach is its failure to consider any possible interaction between the factors, say the failure of one factor to produce the same effect on the response at different levels of another factor. For instance, suppose that two factors A and B affect a response. At one level of A, increasing B causes the response to increase, while at the other level of A, the effect of B totally reverses and the response decreases with increasing B. As interactions exist between electrospinning parameters, this approach may not be an appropriate choice for the case of the present work. The correct strategy to deal with several factors is to use a full factorial design. In this method, factors are all varied together; therefore, all possible combinations of the levels of the factors are investigated. This approach is very efficient, makes the most use of the experimental data and takes into account the interactions between factors [58,59].

It is trivial that in order to draw a line at least two points and for a quadratic curve at least three points are required. Hence, three levels were selected for each parameter in this study so that it would be possible to use quadratic models. These levels were chosen equally spaced. A full factorial experimental design with four factors (solution concentration, spinning distance, applied voltage, and flow rate) each at three levels (3^4 design) were employed resulting in 81 treatment combinations. This design is shown in Fig. 2.

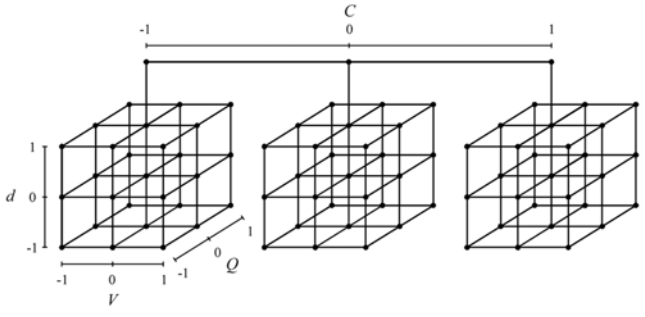

Fig. 2. 3^4 full factorial experimental design used in this study.

−1, 0, and 1 are coded variables corresponding to low, intermediate and high levels of each factor, respectively. The coded variables (x_j) were calculated using Eq. (2) from natural variables (ξ_j). The indices 1 to 4 represent solution concentration, spinning distance, applied voltage, and flow rate, respectively. In addition to experimental data, 15 treatments inside the design space were selected as test data and used for evaluation of the models. The natural and coded variables for experimental data (numbers 1-81) as well as test data (numbers 82-96) are listed in Table 8 in Appendix.

$$x_j = \frac{\xi_j - [\xi_{hj} + \xi_{lj}]/2}{[\xi_{hj} - \xi_{lj}]/2} \tag{2}$$

4. Response Surface Methodology

The mechanism of some scientific phenomena has been well understood and models depicting the physical behavior of the system have been drawn in the form of mathematical relationships. However, there are numerous processes at the moment which have not been sufficiently been understood to permit the theoretical approach. Response surface methodology (RSM) is a combination of mathematical and statistical techniques useful for empirical modeling and analysis of such systems. The application of RSM is in situations where several input variables potentially influence some performance measure or quality characteristic of the process - often called responses. The relationship between the response (y) and k input variables (ξ_1, ξ_2, ..., ξ_k) could be expressed in terms of mathematical notations as follows:

$$y = f(\xi_1, \xi_2, \ldots, \xi_k) \tag{3}$$

where the true response function f is unknown. It is often convenient to use coded variables ($x_1, x_2, \ldots, x_k$) instead of natural (input) variables. The response function will then be:

$$y = f(x_1, x_2, \ldots, x_k) \tag{4}$$

Since the form of the true response function f is unknown, it must be approximated. Therefore, the successful use of RSM is critically dependent upon the choice of appropriate function to approximate f. Low-order polynomials are widely used as approximating functions. First order (linear) models are unable to capture the interaction between parameters, which is a form of curvature in the true response function. Second order (quadratic) models will be likely to perform well in these circumstances. In general, the quadratic model is in the form of:

$$y = \beta_o + \sum_{j=1}^{k} \beta_j x_j + \sum_{j=1}^{k} \beta_{jj} x_j^2 + \sum_{i<j}^{k} \sum_{j=2}^{k} \beta_{ij} x_i x_j + \varepsilon \tag{5}$$

where ε is the error term in the model. The use of polynomials of higher order is also possible but infrequent. The βs are a set of unknown coefficients needed to be estimated. To do that, the first step is to make some observations on the system being studied. The model in Eq. (5) may now be written in matrix notations as:

$$\mathbf{y} = \mathbf{X}\beta + \varepsilon \tag{6}$$

where $\mathbf{y}$ is the vector of observations, $\mathbf{X}$ is the matrix of levels of the variables, β is the vector of unknown coefficients, and ε is the vector of random errors. Afterwards, method of least squares, which minimizes the sum of squares of errors, is employed to find the estimators of the coefficients ($\hat{\beta}$) through:

$$\hat{\beta}=(\mathbf{X}'\mathbf{X})^{-1}\mathbf{X}'\mathbf{y} \quad (7)$$

The fitted model will then be written as:

$$\hat{\mathbf{y}}=\mathbf{X}\hat{\beta} \quad (8)$$

Finally, response surfaces or contour plots are depicted to help visualize the relationship between the response and the variables and see the influence of the parameters [60,61]. As you might notice, there is a close connection between RSM and linear regression analysis [62].

In this study, RSM was employed to establish empirical relationships between four electrospinning parameters (solution concentration, spinning distance, applied voltage, and flow rate) and two responses (mean fiber diameter and standard deviation of fiber diameter). Coded variables were used to build the models. The choice of three levels for each factor in experimental design allowed us to take advantage of quadratic models. Afterwards, the significance of terms in each model was investigated by testing hypotheses on individual coefficients, and simpler yet more efficient models were obtained by eliminating statistically unimportant terms. Finally, the validity of the models was evaluated by using the 15 test data. The analyses were carried out using statistical software Minitab 15.

RESULTS AND DISCUSSION

After the unknown coefficients (βs) were estimated by least squares method, the quadratic models for the mean fiber diameter (MFD) and standard deviation of fiber diameter (StdFD) in terms of coded variables were written as:

$$\begin{aligned}\text{MFD}=&282.031+34.953x_1+5.622x_2-2.113x_3+9.013x_4-11.613x_1^2\\&-4.304x_2^2-15.500x_3^2-0.414x_4^2+12.517x_1x_2+4.020x_1x_3\\&-0.162x_1x_4+20.643x_2x_3+0.741x_2x_4+0.877x_3x_4\end{aligned} \quad (9)$$

$$\begin{aligned}\text{StdFD}=&36.1574+4.5788x_1-1.5536x_2+6.4012x_3+1.1531x_4\\&-2.2937x_1^2-0.1115x_2^2-1.1891x_3^2+3.0980x_4^2\\&-0.2088x_1x_2+1.0010x_1x_3+2.7978x_1x_4+0.1649x_2x_3\\&-2.4876x_2x_4+1.5182x_3x_4\end{aligned} \quad (10)$$

In the next step, a couple of very important hypothesis-testing procedures were carried out to measure the usefulness of the models presented here. First, the test for significance of the model was performed to determine whether there is a subset of variables which contributes significantly in representing the response variations. The appropriate hypotheses are:

$$\begin{aligned}&H_0: \beta_1=\beta_2=\cdots=\beta_k\\&H_1: \beta_j\neq 0 \quad \text{for at least one j}\end{aligned} \quad (11)$$

The F statistics (the result of dividing the factor mean square by the error mean square) of this test along with the *p*-values (a measure of statistical significance, the smallest level of significance for which the null hypothesis is rejected) for both models are shown in Table 1.

Table 1. Summary of the results from statistical analysis of the models

	F	*p*-value	R^2	R^2_{adj}	R^2_{pred}
MFD	106.02	0.000	95.74%	94.84%	93.48%
StdFD	42.05	0.000	89.92%	87.78%	84.83%

The *p*-values of the models are very small (almost zero), so it could be concluded that the null hypothesis is rejected in both cases, suggesting that there are some significant terms in each model. There are also included in Table 1, the values of R^2, R^2_{adj}, and R^2_{pred}. R^2 is a measure for the amount of response variation, which is explained by variables and will always increase when a new term is added to the model regardless of whether the inclusion of the additional term is statistically significant or not. R^2_{adj} is the adjusted form of R^2 for the number of terms in the model; therefore it will increase only if the new terms improve the model and decrease if unnecessary terms are added. R^2_{pred} implies how well the model predicts the response for new observations, whereas R^2 and R^2_{adj} indicate how well the model fits the experimental data. The R^2 values demonstrate that 95.74% of MFD and 89.92% of StdFD are explained by the variables. The R^2_{adj} values are 94.84% and 87.78% for MFD and StdFD, respectively, which accounts for the number of terms in the models. Both R^2 and R^2_{adj} values indicate that the models fit the data very well. The slight difference between the values of R^2 and R^2_{adj} suggests that there might be some insignificant terms in the models. Since the R^2_{pred} values are so close to the values of R^2 and R^2_{adj}, models do not appear to be overfit and have very good predictive ability.

The second testing hypothesis is evaluation of individual coefficients, which would be useful for determination of variables in the models. The hypotheses for testing of the significance of any individual coefficient are:

$$\begin{aligned}&H_0: \beta_j=0\\&H_1: \beta_j\neq 0\end{aligned} \quad (12)$$

The model might be more efficient with inclusion or perhaps exclusion of one or more variables. Therefore, the value of each term in the model is evaluated using this test, and then eliminating the statistically insignificant terms, more efficient models could be obtained. The results of this test for the models of MFD and StdFD are summarized in Table 2 and Table 3, respectively. T statistic in these tables is a measure of the difference between an observed statistic and its hypothesized population value in units of standard error.

Table 2. The test on individual coefficients for the model of mean fiber diameter (MFD)

Term (coded)	Coef	T	*p*-value
Constant	282.031	102.565	0.000
C	34.953	31.136	0.000
d	5.622	5.008	0.000
V	−2.113	−1.882	0.064
Q	9.013	8.028	0.000
C^2	−11.613	−5.973	0.000
d^2	−4.304	−2.214	0.030
V^2	−15.500	−7.972	0.000
Q^2	−0.414	−0.213	0.832
Cd	12.517	9.104	0.000
CV	4.020	2.924	0.005
CQ	−0.162	−0.118	0.906
dV	20.643	15.015	0.000
dQ	0.741	0.539	0.592
VQ	0.877	0.638	0.526

Table 3. The test on individual coefficients for the model of standard deviation of fiber diameter (StdFD)

Term (coded)	Coef	T	*p*-value
Constant	36.1574	39.381	0.000
C	4.5788	12.216	0.000
D	−1.5536	−4.145	0.000
V	6.4012	17.078	0.000
Q	1.1531	3.076	0.003
C^2	−2.2937	−3.533	0.001
d^2	−0.1115	−0.172	0.864
V^2	−1.1891	−1.832	0.072
Q^2	3.0980	4.772	0.000
Cd	−0.2088	−0.455	0.651
CV	1.0010	2.180	0.033
CQ	2.7978	6.095	0.000
dV	0.1649	0.359	0.721
dQ	−2.4876	−5.419	0.000
VQ	1.5182	3.307	0.002

As depicted, the terms related to Q^2, CQ, dQ, and VQ in the model of MFD and related to d^2, Cd, and dV in the model of StdFD have very high *p*-values; therefore, they do not contribute significantly in representing the variation of the corresponding response. Eliminating these terms will enhance the efficiency of the models. The new models are then given by recalculating the unknown coefficients in terms of coded variables in Eqs. (13) and (14), and in terms of natural (uncoded) variables in Eqs. (15), (16).

$$MFD=281.755+34.953x_1+5.622x_2-2.113x_3+9.013x_4 -11.613x_1^2-4.304x_2^2-15.500x_3^2 +12.517x_1x_2+4.020x_1x_3+20.643x_2x_3 \quad (13)$$

$$StdFD=36.083+4.579x_1-1.554x_2+6.401x_3+1.153x_4 -2.294x_1^2-1.189x_3^2+3.098x_4^2 +1.001x_1x_3+2.798x_1x_4-2.488x_2x_4+1.518x_3x_4 \quad (14)$$

$$MFD=10.3345+48.7288C-22.7420d+7.9713V+90.1250Q -2.9033C^2-0.1722d^2-0.6120V^2 +1.2517Cd+0.4020CV+0.8257dV \quad (15)$$

$$StdFD=-1.8823+7.5590C+1.1818d+1.2709V-300.3410Q -0.5734C^2-0.0476V^2+309.7999Q^2+0.1001CV +13.9892CQ-4.9752dQ+3.0364VQ \quad (16)$$

The results of the test for significance as well as R^2, R^2_{adj}, and R^2_{pred} for the new models are given in Table 4. It is obvious that the *p*-values for the new models are close to zero, indicating the existence of some significant terms in each model. Comparing the results of this table with Table 1, the F statistic increased for the new models, indicating the improvement of the models after eliminating the insignificant terms. Despite the slight decrease in R^2, the values of R^2_{adj}, and R^2_{pred} increased substantially for the new models. As mentioned earlier, R^2 will always increase with the number of terms in the model. Therefore, smaller R^2 values were expected for the new models, due to the fewer terms. However, this does not necessarily suggest that the previous models were more efficient. Looking at the tables, R^2_{adj}, which provides a more useful tool for comparing the explanatory power of models with different number of terms, increased after eliminating the unnecessary variables. Hence, the new models have the ability to better explain the experimental data. Due to higher R^2_{pred}, the new models also have higher prediction ability. In other words, eliminating the insignificant terms results in simpler models which not only present the experimental data in superior form, but also are more powerful in predicting new conditions. In the study conducted by Yördem et al. [36], despite high reported R^2 values, the presented models seem to be inefficient and uncertain. Some terms in the models had very high *p*-values. For instance, in modeling the mean fiber diameter, *p*-value as high as 0.975 was calculated for cubic concentration term at spinning distance of 16 cm, where half of the terms had *p*-values more than 0.8. This results

Table 4. Summary of the results from statistical analysis of the models after eliminating the insignificant terms

	F	*p*-value	R^2	R^2_{adj}	R^2_{pred}
MFD	155.56	0.000	95.69%	95.08%	94.18%
StdFD	55.61	0.000	89.86%	88.25%	86.02%

Table 5. The test on individual coefficients for the model of mean fiber diameter (MFD) after eliminating the insignificant terms

Term (coded)	Coef	T	*p*-value
Constant	281.755	118.973	0.000
C	34.953	31.884	0.000
d	5.622	5.128	0.000
V	−2.113	−1.927	0.058
Q	9.013	8.221	0.000
C^2	−11.613	−6.116	0.000
d^2	−.304	−.267	0.026
V^2	−15.500	−8.163	0.000
Cd	12.517	9.323	0.000
CV	4.020	2.994	0.004
dV	20.643	15.375	0.000

Table 6. The test on individual coefficients for the model of standard deviation of fiber diameter (StdFD) after eliminating the insignificant terms

Term (coded)	Coef	T	*p*-value
Constant	36.083	45.438	0.000
C	4.579	12.456	0.000
d	−1.554	−4.226	0.000
V	6.401	17.413	0.000
Q	1.153	3.137	0.003
C^2	−2.294	−3.602	0.001
V^2	−.189	−1.868	0.066
Q^2	3.098	4.866	0.000
CV	1.001	2.223	0.029
CQ	2.798	6.214	0.000
dQ	−2.488	−5.525	0.000
VQ	1.518	3.372	0.001

in low R^2_{pred} values which were not reported in their study, and after calculating by us, they were found to be almost zero in many cases suggesting the poor prediction ability of their models.

The test for individual coefficients was performed again for the new models. with the results summarized in Table 5 and Table 6. This time, as it was anticipated, no terms had higher *p*-value than expected, which need to be eliminated. Here is another advantage of removing unimportant terms. The values of T statistic increased for the terms already in the models implying that their effects on the response became stronger.

After developing the relationship between parameters, the test data were used to investigate the prediction ability of the models. Root mean square errors (RMSE) between the calculated responses (C_i) and real responses (R_i) were determined by using Eq. (17) for experimental data as well as test data for the sake of evaluation of both MFD and StdFD models, and the results are listed in Table 7.

Table 7. RMSE values of the models for the experimental and test data

	Experimental data	Test data
MFD	7.489	10.647
StdFD	2.493	2.890

The models present acceptable RMSE values for test data, indicating the ability of the models to generalize well the experimental data to predicting new conditions. Although the values of RMSE for the test data are slightly higher than experimental data, these small discrepancies were expected since it is almost impossible for an empirical model to express the test data as well as experimental data and higher errors are often obtained when new data are presented to the models. Hence, the results imply the acceptable prediction ability of the models.

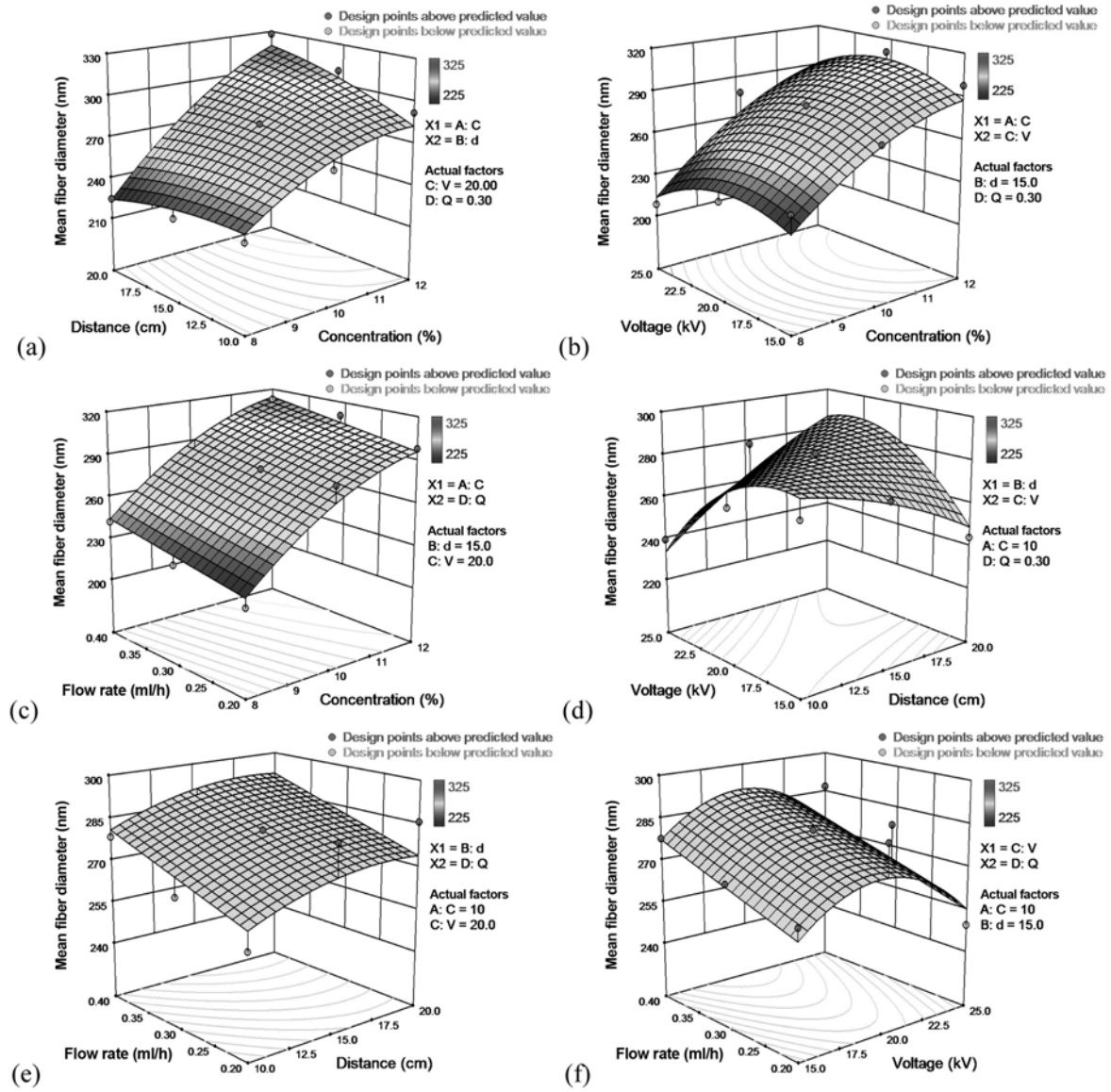

Fig. 3. Response surfaces for mean fiber diameter in terms of: (a) solution concentration and spinning distance, (b) solution concentration and applied voltage, (c) solution concentration and flow rate, (d) spinning distance and applied voltage, (e) spinning distance and flow rate, (f) applied voltage and flow rate.

$$RMSE = \sqrt{\frac{\sum_{i=1}^{n}(C_i - R_i)^2}{n}} \quad (17)$$

1. Response Surfaces for Mean Fiber Diameter

1-1. Solution Concentration

A monotonic increase in MFD with concentration was observed in this study as shown in Fig. 3(a), (b), and (c) which agrees with the previous observations [25,31,63-65]. The concentration effect was more pronounced at further spinning distances (Fig. 3(a)). This could be attributed to the two-fold effect of distance. At low concentrations, higher solvent content in the solution and longer distance provides more time not only to stretch the jet in the electric field but also to evaporate the solvent, thereby encouraging thinner fiber formation. At higher concentrations, however, there are extensive polymer chain entanglements, resulting in higher viscoelastic forces which tend to resist against the electrostatic stretching force. On the other hand, increasing the spinning distance will reduce the electric field strength (E=V/d) causing the electrostatic force to decrease. As a result, increasing MFD with concentration gains more momentum at longer spinning distances. Higher applied voltages also accelerate the concentration impact on MFD (Fig. 3(b)), which may be ascribed to the two-fold effect of voltage. At higher voltages, where the electric field is strong and dominant factor, increasing polymer concentration tends to encourage the effect of voltage on mass flow rate of polymer. Hence, more solution could be removed from the tip of the needle, resulting in further increase in MFD. No combined effect between solution concentration and volume flow rate was observed, as depicted in Fig. 3(c). Therefore, concentration had interactions with spinning distance and applied voltage which had been suggested by the existence of terms Cd and CV in the model of MFD. Recall that the term CQ was statistically insignificant and therefore had been removed from the model of MFD.

1-2. Spinning Distance

The impact of spinning distance on MFD is illustrated in Fig. 3(a), (d), and (e). As depicted in these figures, the effect of spinning distance is not always the same. Spinning distance has a two-fold effect on electrospun fiber diameter. Varying the distance has a direct influence on the jet flight time as well as electric field strength. Longer spinning distance will provide more time for the jet to stretch in the electric field before it is deposited on the collector. Furthermore, solvents will have more time to evaporate. Hence, the fiber diameter will be prone to decrease. On the other hand, increasing the spinning distance, the electric field strength will decrease (E=V/d), resulting in less acceleration, hence stretching of the jet which leads to thicker fiber formation. The balance between these two effects will determine the final fiber diameter. Increase in fiber diameter [64,67,68] as well as decrease in fiber diameter [31] with increasing spinning distance was reported in the literature. There were also some cases in which spinning distance did not have a significant influence on fiber diameter [63,69-71]. As mentioned before, there will be more chain entanglements at higher concentrations resulting in an increase in viscoelastic force. Furthermore, the longer the distance, the lower is the electric field strength. The electrostatic stretching force, which has now become weaker, will be dominated easier by the viscoelastic force. As a result, the effect of spinning distance on fiber diameter is more highlighted, rendering higher MFD (Fig. 3(a)). The effect of spinning distance will also alter at different applied voltages (Fig. 3(d)). At low voltages, longer spinning distance brought about thinner fiber formation, whereas at high voltages, the effect of spinning distance was totally reversed and fibers with thicker diameters were obtained at longer distances. It is supposed that at low voltages, the stretching time becomes the dominant factor. Hence, longer spinning distance, which gives more time for jet stretching and thinning and solvent evaporation, will result in fibers with smaller diameters. At high voltages, however, the electric field strength is high and dominant. Therefore, increasing the distance, which reduces the electric field, causes an increase in fiber diameter. The function of spinning distance was observed to be independent of volume flow rate for MFD (Fig. 3(e)). The interaction of spinning distance with solution concentration and applied voltage demonstrated in Fig. 3(a) and (d), proved the existence of terms Cd and dV in the model of MFD.

1-3. Applied Voltage

Fig. 3(b), (d), and (f) show the effect of applied voltage on MFD. Increasing the voltage resulted in an increase followed by a decrease in MFD. Applied voltage has two major different effects on fiber diameter. Firstly, increasing the applied voltage will increase the electric field strength and larger electrostatic stretching force causes the jet to accelerate more in the electric field, thereby favoring thinner fiber formation. Secondly, since charge transport is only carried out by the flow of polymer in the electrospinning process [72], increasing the voltage would induce more surface charges on the jet. Subsequently, the mass flow rate from the needle tip to the collector will increase, say the solution will be drawn more quickly from the tip of the needle causing fiber diameter to increase. The combination of these two effects will determine the final fiber diameter. Hence, increasing applied voltage may decrease [73-75], increase [63,64,68] or may not change [25,31,69,76] the fiber diameter. According to the given explanation, at low voltages, where the electric field strength is low, the effect of mass of solution could be dominant. Therefore, fiber diameter increases when the applied voltage rises. However, as the voltage exceeds a limit, the electric field will be high enough to be a determining factor. Hence, fiber diameter decreases as the voltage increases. The effect of voltage on MFD was influenced by solution concentration to some extent (Fig. 3(b)). At high concentrations, the increase in fiber diameter with voltage was more pronounced. This could be attributed to the fact that the effect of mass of solution will be more important for the solutions of higher concentrations. The change in fiber diameter as a function of voltage is dramatically influenced by spinning distance (Fig. 3(d)). At a short distance, the electric field is a high and dominant factor. Therefore, increasing applied voltage, which strengthens the electric field, results in a decrease in fiber diameter. Whereas, at long distances where the electric field is low, the effect of mass of solution would be determining factor according to which fiber diameter increased with applied voltage. The effect of applied voltage on MFD is found to be independent of volume flow rate (Fig. 3(f)). It is quite apparent that there is a huge interaction between applied voltage and spinning distance, a slight interaction between applied voltage and solution concentration and no interaction between applied voltage and volume flow rate, which is in agreement with the presence of CV and dV and absence of VQ in the model of MFD.

1-4. Volume Flow Rate

It was suggested that a minimum value for solution flow rate is required to form the drop of polymer at the tip of the needle for the sake of maintaining a stable Taylor cone [77]. Hence, flow rate could affect the morphology of electrospun nanofibers such as fiber diameter. Increasing the flow rate, more amount of solution is delivered to the tip of the needle enabling the jet to carry the solution away faster. This could bring about an increase in the jet diameter, favoring thicker fiber formation. In this study, the MFD slightly increased with volume flow rate (Fig. 3(c), (e), and (f)) which agrees with the previous researches [31,77-79]. Flow rate was also found to influence MFD independent from solution concentration, applied voltage, and spinning distance as suggested earlier by the absence of CQ, dQ, and VQ in the model of MFD.

2. Response Surfaces for Standard Deviation of Fiber Diameter

2-1. Solution Concentration

As depicted in Fig. 4(a), (b), and (c), StdFD increased with concentration, which is in agreement with the previous observations [25,31,34,63,66,68,80,81]. Increasing the polymer concentration, the macromolecular chain entanglements increase, prompting a greater difficulty for the jet to stretch and split. This could result in less uniform fibers (higher StdFD). Concentration affected StdFD regardless of spinning distance (Fig. 4(a)), suggesting that there was no interaction between these two parameters (absence of Cd in the model of StdFd). At low applied voltages, the formation of more uniform fibers with decreasing the concentration was facilitated. In agreement with existence of the term CV in the model of StdFd, solution concentration was found to have a slight interaction with applied voltage (Fig. 4(b)). The curvature of the surface in Fig. 4(c) suggested that there was a noticeable interaction between concentration and flow rate and this agrees with the presence of the term CQ in the model of StdFD.

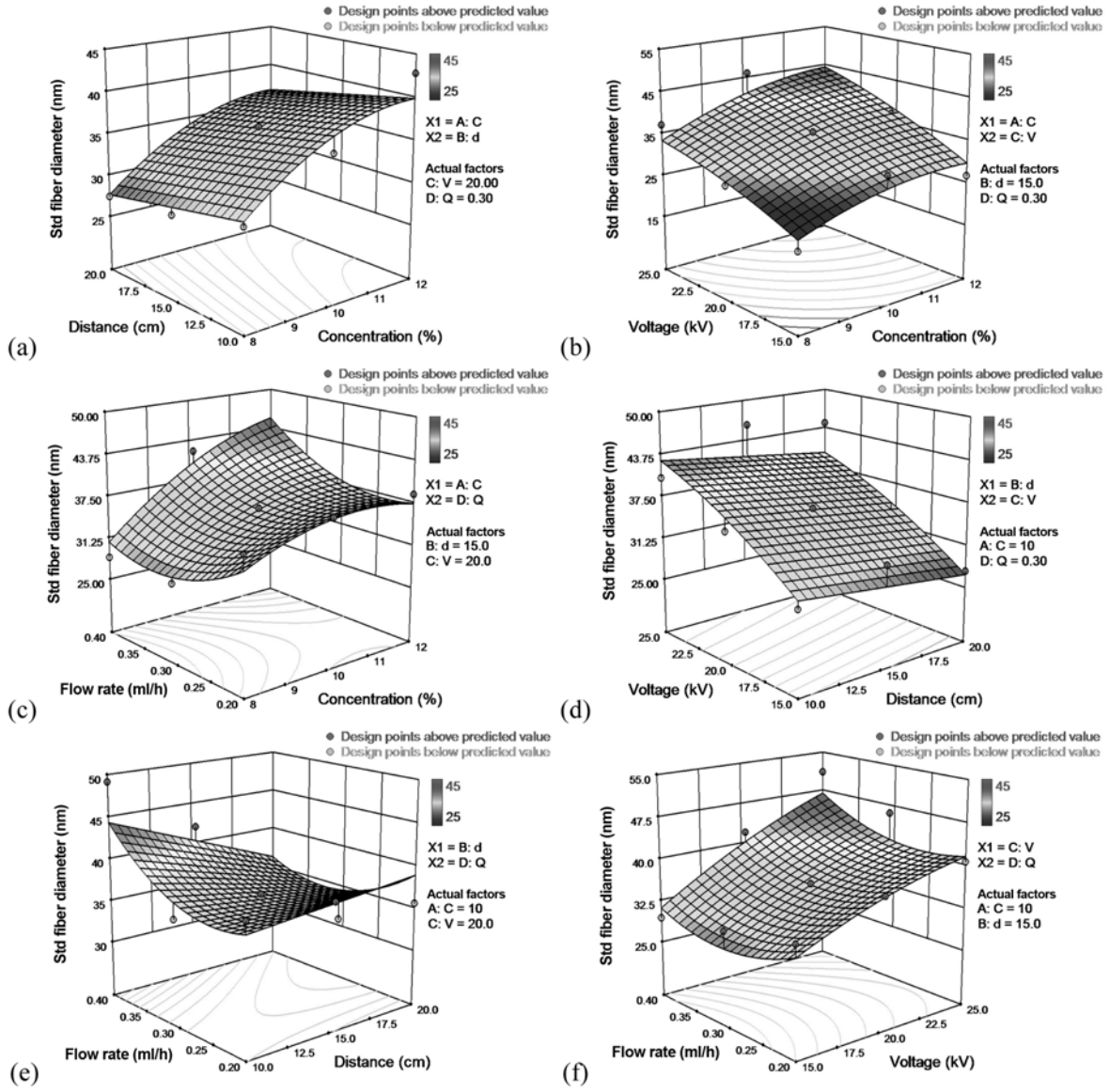

Fig. 4. Response surfaces for standard deviation of fiber diameter in terms of: (a) solution concentration and spinning distance, (b) solution concentration and applied voltage, (c) solution concentration and flow rate, (d) spinning distance and applied voltage, (e) spinning distance and flow rate, (f) applied voltage and flow rate.

2-2. Spinning Distance

More uniform fibers (lower StdFD) were obtained with increasing the spinning distance as shown in Fig. 4(a), (d), and (e). At longer spinning distance, more time is provided for jet flying from the tip of the needle to the collector and solvent evaporation. Therefore, jet stretching and solvent evaporation is carried out more gently, resulting in more uniform fibers. Our finding is consistent with the trend observed by Zhao et al. [81]. Spinning distance influenced StdFD regardless of solution concentration and applied voltage (Fig. 4(a) and (d)), indicating that no interaction exists between these variables as could be inferred from the model of StdFD. However, the interaction of spinning distance with volume flow rate is obvious (Fig. 4(e)). The presence of dQ in the model of StdFD proves this observation. The effect of spinning distance is more highlighted at higher flow rates. This could be attributed to the fact that more solution is delivered to the tip of the needle at higher flow rates; therefore the threads will require more time to dry. If the distance is high enough to provide the sufficient time, uniform fibers will be formed. Decreasing the distance, there will be less time for solvent to evaporate, favoring the production of non-uniform fibers (high StdFD).

2-3. Applied Voltage

StdFD was found to increase with applied voltage (Fig. 4(b), (d), and (f)) as observed in other studies [63,64,68,81]. Increasing the applied voltage causes the effect of the electric field on the charged jet to increase. Hence, the flight speed of the jet increases, shortening the time that the jet travels towards the collector. As a result, less time is provided for jet stretching and thinning and also solvent evaporation. This may result in formation of less uniform fibers (higher StdFD). The effect of applied voltage on StdFD is influenced by solution concentration as shown in Fig. 4(b), implying the interaction of voltage with concentration, which was earlier addressed in the paper by the presence of the corresponding term in the model of StdFD. At low concentrations, the formation of uniform fibers with decreasing the applied voltage was facilitated. No interaction was observed between applied voltage and spinning distance (Fig. 4(d)) as suggested by the absence of the term dV in the model of StdFD. Fig. 4(f) shows a slight interaction of voltage with flow rate, which concurs with the existence of VQ in the model of StdFD.

2-4. Volume Flow Rate

As demonstrated in Fig. 4(c), (e), and (f), the uniformity of fibers increased (StdFD decreased), reached to an optimum value and then decreased (StdFD increased) by increasing of the flow rate. When the flow rate is low, the amount of solution fed to the tip of the needle is not sufficient, whereas an excess amount of solution is delivered to the tip of the needle at high flow rates. Unstable jets are formed in the two extremes resulting in the production of non-uniform fibers. The impact of flow rate on StdFD is influenced by solution concentration, applied voltage, and spinning distance. This observation indicates the interaction between flow rate and other variables as demonstrated by the terms CQ, dQ, and VQ in the model of StdFD. Increasing the solution concentration favored the formation of non-uniform fibers at high flow rates (Fig. 4(c)), which is probably the outcome of greater difficulty of solution removal. The effect of flow rate on StdFD was more pronounced as the spinning distance decreased (Fig. 4(e)). The shorter the distance, the less the time provided to the jet to thin and dry. Therefore, at high flow rates, more amount of solution is delivered with insufficient flying time, results in formation of less uniform fibers. High applied voltage encouraged the increase in StdFD at fast flow rates as depicted in Fig. 4(f).

CONCLUSION

The simultaneous effects of four processing variables, including solution concentration, applied voltage, spinning distance, and volume flow rate on MFD and StdFD, were investigated quantitatively and qualitatively. The appropriate range of parameters where dry, bead-free, and continuous fibers without breaking up to droplets are formed, was selected by referring to the literature along with conducting a series of preliminary experiments. A full factorial experimental design at three levels of each factor (3^4 design) was carried out. Moreover, 15 treatments inside the design space were selected as test set for evaluating the prediction ability of the models. PVA Nanofibers were then prepared for experimental and test sets through the electrospinning method. After that, MFD and StdFD were determined from SEM micrograph of each sample. RSM was used to establish quadratic models for MFD and StdFD. The test for significance of the coefficients demonstrated that the terms Q^2, CQ, dQ, and VQ in the model of MFD and d^2, Cd, and dV in the model of StdFD were not of important value in representing the responses. Eliminating these terms, simpler yet more efficient models were obtained which not only explained the experimental data in a better manner, but also had more prediction ability. Afterwards, in order to show the generalization ability of the models for predicting new conditions, the test set was used. Low RMSE of test set for MFD and StdFD were obtained, indicating the good prediction ability of the models. Finally, in order to qualitatively study the effects of variables on MFD and StdFD, response surface plots were generated by using the obtained relationships.

For MFD:

1. Increasing solution concentration, MFD increased rigorously. The effect of concentration was more pronounced at longer spinning distance and also at higher applied voltage.

2. The effect of spinning distance on MFD changed depending on solution concentration and applied voltage. At low applied voltages, MFD decreased as the spinning distance became longer, whereas higher MFD resulted with lengthening the spinning distance when the applied voltage was high. Increasing the solution concentration tended to assist the formation of thicker fibers at longer spinning distance.

3. Raising the applied voltage, MFD was observed to first increase and then decrease. High solution concentrations partly and long spinning distances largely favored the increase of MFD with applied voltage.

4. MFD slightly increased with flow rate. The impact of flow rate on MFD was unrelated to the other variables.

For StdFD:

1. The higher the solution concentration, the less uniform fibers (higher StdFD) was formed. Low applied voltages facilitated the formation of more uniform fibers (lower StdFD) with decreasing the concentration. The increase of StdFD with concentration gained momentum at high flow rates.

2. Longer spinning distance resulted in more uniform fibers (lower StdFD). The effect of spinning distance was more pronounced at higher flow rates.

3. Raising the applied voltage increased StdFD. Low concentrations facilitated the formation of uniform fibers (high StdFD) with decreasing the applied voltage.

4. Flow rate was found to have a significant impact on uniformity of fibers (StdFD). As flow rate increased, StdFD decreased and then increased. Higher solution concentration, higher applied voltage, and shorter spinning distance encouraged the formation of non-uniform fibers (high StdFD) at fast flow rates.

REFERENCES

1. G. I. Taylor, *Proc. Roy. Soc.* London, **313**, 453 (1969).
2. J. Doshi and D. H. Reneker, *J. Electrostatics*, **35**, 151 (1995).
3. H. Fong and D. H. Reneker, *Electrospinning and the formation of nanofibers*, in: D. R. Salem (Ed.), Structure formation in polymeric fibers, Hanser, Cincinnati (2001).
4. D. Li and Y. Xia, *Adv. Mater.*, **16**, 1151 (2004).
5. R. Derch, A. Greiner and J. H. Wendorff, *Polymer nanofibers prepared by electrospinning*, in: J. A. Schwarz, C. I. Contescu and K. Putyera (Eds.), Dekker encyclopedia of nanoscience and nanotechnology, CRC, New York (2004).
6. A. K. Haghi and M. Akbari, *Phys. Stat. Sol. A*, **204**, 1830 (2007).
7. P. W. Gibson, H. L. Schreuder-Gibson and D. Rivin, *AIChE J.*, **45**, 190 (1999).
8. M. Ziabari, V. Mottaghitalab and A. K. Haghi, *Korean J. Chem. Eng.*, **25**, 923 (2008).
9. Z. M. Huang, Y. Z. Zhang, M. Kotaki and S. Ramakrishna, *Compos. Sci. Technol.*, **63**, 2223 (2003).
10. M. Li, M. J. Mondrinos, M. R. Gandhi, F. K. Ko, A. S. Weiss and P. I. Lelkes, *Biomaterials*, **26**, 5999 (2005).
11. E. D. Boland, B. D. Coleman, C. P. Barnes, D. G. Simpson, G. E. Wnek and G. L. Bowlin, *Acta Biomater.*, **1**, 115 (2005).
12. J. Lannutti, D. Reneker, T. Ma, D. Tomasko and D. Farson, *Mater. Sci. Eng. C*, **27**, 504 (2007).
13. J. Zeng, L. Yang, Q. Liang, X. Zhang, H. Guan, C. Xu, X. Chen and X. Jing, *J. Control. Release*, **105**, 43 (2005).
14. E. R. Kenawy, G. L. Bowlin, K. Mansfield, J. Layman, D. G. Simpson, E. H. Sanders and G. E. Wnek, *J. Control. Release*, **81**, 57 (2002).
15. M. S. Khil, D. I. Cha, H.-Y. Kim, I.-S. Kim and N. Bhattarai, *J. Biomed. Mater. Res. Part B: Appl. Biomater.*, **67**, 675 (2003).
16. B. M. Min, G. Lee, S. H. Kim, Y. S. Nam, T. S. Lee and W. H. Park, *Biomaterials*, **25**, 1289 (2004).
17. X. H. Qin and S. Y. Wang, *J. Appl. Polym. Sci.*, **102**, 1285 (2006).
18. H. S. Park and Y. O. Park, *Korean J. Chem. Eng.*, **22**, 165 (2005).
19. J. S. Kim and D. H. Reneker, *Poly. Eng. Sci.*, **39**, 849 (1999).
20. S. W. Lee, S. W. Choi, S. M. Jo, B. D. Chin, D. Y. Kim and K. Y. Lee, *J. Power Sources*, **163**, 41 (2006).
21. C. Kim, *J. Power Sources*, **142**, 382 (2005).
22. N. J. Pinto, A. T. Johnson, A. G. MacDiarmid, C. H. Mueller, N. Theofylaktos, D. C. Robinson and F. A. Miranda, *Appl. Phys. Lett.*, **83**, 4244 (2003).
23. D. Aussawasathien, J.-H. Dong and L. Dai, *Synthetic Met.*, **54**, 37 (2005).
24. S.-Y. Jang, V. Seshadri, M.-S. Khil, A. Kumar, M. Marquez, P. T. Mather and G. A. Sotzing, *Adv. Mater.*, **17**, 2177 (2005).
25. S.-H. Tan, R. Inai, M. Kotaki and R. Ramakrishna, *Polymer*, **46**, 6128 (2005).
26. A. Ziabicki, *Fundamentals of fiber formation: The science of fiber spinning and drawing*, Wiley, New York (1976).
27. A. Podgóski, A. Bałazy and L. Gradoń, *Chem. Eng. Sci.*, **61**, 6804 (2006).
28. B. Ding, M. Yamazaki and S. Shiratori, *Sens. Actuators B*, **106**, 477 (2005).
29. J. R. Kim, S. W. Choi, S. M. Jo, W. S. Lee and B. C. Kim, *Electrochim. Acta*, **50**, 69 (2004).
30. L. Moroni, R. Licht, J. de Boer, J. R. de Wijn and C. A. van Blitterswijk, *Biomaterials*, **27**, 4911 (2006).
31. T. Wang and S. Kumar, *J. Appl. Polym. Sci.*, **102**, 1023 (2006).
32. W. Cui, X. Li, S. Zhou and J. Weng, *J. Appl. Polym. Sci.*, **103**, 3105 (2007).
33. S. Sukigara, M. Gandhi, J. Ayutsede, M. Micklus and F. Ko, *Polymer*, **45**, 3701 (2004).
34. S. Y. Gu, J. Ren and G. J. Vancso, *Eur. Polym. J.*, **41**, 2559 (2005).
35. S. Y. Gu and J. Ren, *Macromol. Mater. Eng.*, **290**, 1097 (2005).
36. O. S. Yördem, M. Papila and Y. Z. Menceloğlu, *Mater. Design*, **29**, 34 (2008).
37. I. Sakurada, *Polyvinyl alcohol fibers*, CRC, New York (1985).
38. F. L. Marten, *Vinyl alcohol polymers*, in: H. F. Mark (Ed.), Encyclopedia of polymer science and technology, 3rd ed., vol. 8, Wiley (2004).
39. Y. D. Kwon, S. Kavesh and D. C. Prevorsek, U.S. Patent, 4,440,711 (1984).
40. S. Kavesh and D. C. Prevorsek, U.S. Patent, 4,551,296 (1985).
41. H. Tanaka, M. Suzuki and F. Uedo, U.S. Patent, 4,603,083 (1986).
42. G. Paradossi, F. Cavalieri, E. Chiessim, C. Spagnoli and M. K. Cowman, *J. Mater. Sci.: Mater. Med.*, **14**, 687 (2003).
43. G. Zheng-Qiu, X. Jiu-Mei and Z. Xiang-Hong, *Biomed. Mater. Eng.*, **8**, 75 (1998).
44. M. Oka, K. Ushio, P. Kumar, K. Ikeuchi, S. H. Hyon, T. Nakamura and H. Fujita, *P. I. Mech. Eng. H*, **214**, 59 (2000).
45. K. Burczak, E. Gamian and A. Kochman, *Biomaterials*, **17**, 2351 (1996).
46. J. K. Li, N. Wang and X. S. Wu, *J. Control. Release*, **56**, 117 (1998).
47. A. S. Hoffman, *Adv. Drug Delivery Rev.*, **43**, 3 (2002).
48. J. Zeng, A. Aigner, F. Czubayko, T. Kissel, J. H. Wendorff and A. Greiner, *Biomacromolecules*, **6**, 1484 (2005).
49. K. H. Hong, *Polym. Eng. Sci.*, **47**, 43 (2007).
50. M. Ziabari, V. Mottaghitalab and A. K. Haghi, *Korean J. Chem. Eng.*, **25**, 919 (2008).
51. M. Ziabari, V. Mottaghitalab and A. K. Haghi, *Braz. J. Chem. Eng.*, **26**, 53 (2009).
52. M. Ziabari, V. Mottaghitalab, S. T. McGovern and A. K. Haghi, *Nanoscale Res. Lett.*, **2**, 597 (2007).
53. M. Ziabari, V. Mottaghitalab and A. K. Haghi, *Korean J. Chem. Eng.*, **25**, 905 (2008).
54. L. H. Sperling, *Introduction to physical polymer science*, 4th ed., Wiley, New Jersey (2006).
55. J. C. J. F. Tacx, H. M. Schoffeleers, A. G. M. Brands and L. Teuwen, *Polymer*, **41**, 947 (2000).
56. F. K. Ko, *Nanofiber technology*, in: Y. Gogotsi (Ed.), Nanomaterials handbook, CRC, Boca Raton (2006).
57. A. Koski, K. Yim and S. Shivkumar, *Mater. Lett.*, **58**, 493 (2004).
58. D. C. Montgomery, *Design and analysis of experiments*, 5th ed.,

Wiley, New York (1997).
59. A. Dean and D. Voss, *Design and analysis of experiments*, Springer, New York (1999).
60. G. E. P. Box and N. R. Draper, *Response surfaces, mixtures, and ridge analyses*, Wiley, New Jersey (2007).
61. K. M. Carley, N. Y. Kamneva and J. Reminga, *Response surface methodology*, CASOS Technical Report, CMU-ISRI-04-136 (2004).
62. S. Weisberg, *Applied linear regression*, 3rd ed., Wiley, New Jersey (2005).
63. C. Zhang, X. Yuan, L. Wu, Y. Han and J. Sheng, *Eur. Polym. J.*, **41**, 423 (2005).
64. Q. Li, Z. Jia, Y. Yang, L. Wang and Z. Guan, *Preparation and properties of poly(vinyl alcohol) nanofibers by electrospinning*, Proceedings of IEEE International Conference on Solid Dielectrics, Winchester, U.K. (2007).
65. C. Mit-uppatham, M. Nithitanakul and P. Supaphol, *Macromol. Chem. Phys.*, **205**, 2327 (2004).
66. Y. J. Ryu, H. Y. Kim, K. H. Lee, H. C. Park and D. R. Lee, *Eur. Polym. J.*, **39**, 1883 (2003).
67. T. Jarusuwannapoom, W. Hongrojjanawiwat, S. Jitjaicham, L. Wannatong, M. Nithitanakul, C. Pattamaprom, P. Koombhongse, R. Rangkupan and P. Supaphol, *Eur. Polym. J.*, **41**, 409 (2005).
68. S. C. Baker, N. Atkin, P. A. Gunning, N. Granville, K. Wilson, D. Wilson and J. Southgate, *Biomaterials*, **27**, 3136 (2006).
69. S. Sukigara, M. Gandhi, J. Ayutsede, M. Micklus and F. Ko, *Polymer*, **44**, 5721 (2003).
70. X. Yuan, Y. Zhang, C. Dong and J. Sheng, *Polym. Int.*, **53**, 1704 (2004).
71. C. S. Ki, D. H. Baek, K. D. Gang, K. H. Lee, I. C. Um and Y. H. Park, *Polymer*, **46**, 5094 (2005).
72. J. M. Deitzel, J. Kleinmeyer, D. Harris and N. C. Beck Tan, *Polymer*, **42**, 261 (2001).
73. C. J. Buchko, L. C. Chen, Y. Shen and D. C. Martin, *Polymer*, **40**, 7397 (1999).
74. J. S. Lee, K. H. Choi, H. D. Ghim, S. S. Kim, D. H. Chun, H. Y. Kim and W. S. Lyoo, *J. Appl. Polym. Sci.*, **93**, 1638 (2004).
75. S. F. Fennessey and R. J. Farris, *Polymer*, **45**, 4217 (2004).
76. S. Kidoaki, I. K. Kwon and T. Matsuda, *Biomaterials*, **26**, 37 (2005).
77. X. Zong, K. Kim, D. Fang, S. Ran, B. S. Hsiao and B. Chu, *Polymer*, **43**, 4403 (2002).
78. D. Li and Y. Xia, *Nano. Lett.*, **3**, 555 (2003).
79. W.-Z. Jin, H.-W. Duan, Y.-J. Zhang and F.-F. Li, *Nonafiber membrane of EVOH-based ionomer by electrospinning*, Proceedings of the 1st IEEE International Conference on Nano/Micro Engineered and Molecular Systems, Zhuhai, China (2006).
80. X. M. Mo, C. Y. Xu, M. Kotaki and S. Ramakrishna, *Biomaterials*, **25**, 1883 (2004).
81. S. Zhao, X. Wu, L. Wang and Y. Huang, *J. Appl. Polym. Sci.*, **91**, 242 (2004).

APPENDIX

Table 8. Natural and coded variables for experimental and test data along with corresponding responses

No.	Natural variables				Coded variables				Responses	
	C (%)	d (cm)	V (kV)	Q (ml/h)	x_1	x_2	x_3	x_4	MFD (nm)	StdFD (nm)
1	8	10	15	0.2	−1	−1	−1	−1	232.62	26.60
2	8	10	15	0.3	−1	−1	−1	0	235.50	24.52
3	8	10	15	0.4	−1	−1	−1	1	252.02	25.89
4	8	10	20	0.2	−1	−1	0	−1	236.84	37.30
5	8	10	20	0.3	−1	−1	0	0	232.08	30.22
6	8	10	20	0.4	−1	−1	0	1	249.21	34.49
7	8	10	25	0.2	−1	−1	1	−1	196.05	34.76
8	8	10	25	0.3	−1	−1	1	0	201.38	35.15
9	8	10	25	0.4	−1	−1	1	1	215.00	39.00
10	8	15	15	0.2	−1	0	−1	−1	221.10	28.88
11	8	15	15	0.3	−1	0	−1	0	238.63	20.17
12	8	15	15	0.4	−1	0	−1	1	242.32	21.99
13	8	15	20	0.2	−1	0	0	−1	219.76	36.19
14	8	15	20	0.3	−1	0	0	0	228.56	28.29
15	8	15	20	0.4	−1	0	0	1	242.01	28.30
16	8	15	25	0.2	−1	0	1	−1	202.62	33.22
17	8	15	25	0.3	−1	0	1	0	208.21	37.14
18	8	15	25	0.4	−1	0	1	1	213.66	34.84
19	8	20	15	0.2	−1	1	−1	−1	196.63	30.69
20	8	20	15	0.3	−1	1	−1	0	197.73	24.55
21	8	20	15	0.4	−1	1	−1	1	206.28	22.11
22	8	20	20	0.2	−1	1	0	−1	206.69	31.56
23	8	20	20	0.3	−1	1	0	0	224.38	27.41
24	8	20	20	0.4	−1	1	0	1	242.06	26.51

Table 8. Continued

No.	Natural variables				Coded variables				Responses	
	C (%)	d (cm)	V (kV)	Q (ml/h)	x_1	x_2	x_3	x_4	MFD (nm)	StdFD (nm)
25	8	20	25	0.2	−1	1	1	−1	205.25	40.32
26	8	20	25	0.3	−1	1	1	0	215.70	30.54
27	8	20	25	0.4	−1	1	1	1	231.34	32.40
28	10	10	15	0.2	0	−1	−1	−1	269.91	30.35
29	10	10	15	0.3	0	−1	−1	0	270.05	28.88
30	10	10	15	0.4	0	−1	−1	1	291.99	33.98
31	10	10	20	0.2	0	−1	0	−1	256.11	38.54
32	10	10	20	0.3	0	−1	0	0	264.86	35.70
33	10	10	20	0.4	0	−1	0	1	278.34	49.13
34	10	10	25	0.2	0	−1	1	−1	228.21	42.33
35	10	10	25	0.3	0	−1	1	0	239.28	40.30
36	10	10	25	0.4	0	−1	1	1	238.74	46.57
37	10	15	15	0.2	0	0	−1	−1	263.67	34.16
38	10	15	15	0.3	0	0	−1	0	269.29	31.54
39	10	15	15	0.4	0	0	−1	1	277.71	29.40
40	10	15	20	0.2	0	0	0	−1	284.20	38.18
41	10	15	20	0.3	0	0	0	0	281.82	36.27
42	10	15	20	0.4	0	0	0	1	282.39	42.07
43	10	15	25	0.2	0	0	1	−1	249.42	40.79
44	10	15	25	0.3	0	0	1	0	278.22	46.15
45	10	15	25	0.4	0	0	1	1	286.96	51.16
46	10	20	15	0.2	0	1	−1	−1	239.45	27.98
47	10	20	15	0.3	0	1	−1	0	244.04	27.43
48	10	20	15	0.4	0	1	−1	1	251.58	27.26
49	10	20	20	0.2	0	1	0	−1	285.67	35.62
50	10	20	20	0.3	0	1	0	0	273.05	30.74
51	10	20	20	0.4	0	1	0	1	280.62	34.66
52	10	20	25	0.2	0	1	1	−1	278.10	40.79
53	10	20	25	0.3	0	1	1	0	280.95	44.58
54	10	20	25	0.4	0	1	1	1	306.28	44.04
55	12	10	15	0.2	1	−1	−1	−1	286.23	27.12
56	12	10	15	0.3	1	−1	−1	0	295.60	32.91
57	12	10	15	0.4	1	−1	−1	1	293.41	40.48
58	12	10	20	0.2	1	−1	0	−1	271.20	34.86
59	12	10	20	0.3	1	−1	0	0	291.89	42.78
60	12	10	20	0.4	1	−1	0	1	295.93	49.43
61	12	10	25	0.2	1	−1	1	−1	234.13	39.31
62	12	10	25	0.3	1	−1	1	0	247.65	48.60
63	12	10	25	0.4	1	−1	1	1	247.13	59.02
64	12	15	15	0.2	1	0	−1	−1	271.93	33.05
65	12	15	15	0.3	1	0	−1	0	297.65	26.75
66	12	15	15	0.4	1	0	−1	1	296.79	39.84
67	12	15	20	0.2	1	0	0	−1	297.94	38.82
68	12	15	20	0.3	1	0	0	0	310.06	36.84
69	12	15	20	0.4	1	0	0	1	312.15	41.69
70	12	15	25	0.2	1	0	1	−1	272.24	39.55
71	12	15	25	0.3	1	0	1	0	282.04	42.35
72	12	15	25	0.4	1	0	1	1	288.00	51.72
73	12	20	15	0.2	1	1	−1	−1	259.63	34.63
74	12	20	15	0.3	1	1	−1	0	278.40	25.35
75	12	20	15	0.4	1	1	−1	1	279.25	27.25

Table 8. Continued

No.	Natural variables				Coded variables				Responses	
	C (%)	d (cm)	V (kV)	Q (ml/h)	x_1	x_2	x_3	x_4	MFD (nm)	StdFD (nm)
76	12	20	20	0.2	1	1	0	−1	307.42	42.25
77	12	20	20	0.3	1	1	0	0	327.77	35.71
78	12	20	20	0.4	1	1	0	1	337.88	45.16
79	12	20	25	0.2	1	1	1	−1	321.78	46.21
80	12	20	25	0.3	1	1	1	0	334.54	40.68
81	12	20	25	0.4	1	1	1	1	342.45	47.94
82	9	20	15	0.3	−0.5	1	−1	0	216.53	24.25
83	10	12.5	15	0.3	0	−0.5	−1	0	259.61	25.67
84	10	20	22.5	0.3	0	1	0.5	0	300.27	35.71
85	10	20	15	0.25	0	1	−1	−0.5	235.04	29.64
86	9	12.5	15	0.3	−0.5	−0.5	−1	0	247.57	26.65
87	9	20	22.5	0.3	−0.5	1	0.5	0	247.16	31.12
88	9	20	15	0.25	−0.5	1	−1	−0.5	212.82	30.26
89	10	12.5	22.5	0.3	0	−0.5	0.5	0	263.70	45.06
90	10	12.5	15	0.25	0	−0.5	−1	−0.5	258.26	26.16
91	10	20	22.5	0.25	0	1	0.5	−0.5	272.03	36.28
92	9	12.5	22.5	0.3	−0.5	−0.5	0.5	0	235.75	33.16
93	9	12.5	15	0.25	−0.5	−0.5	−1	−0.5	244.43	24.87
94	9	20	22.5	0.25	−0.5	1	0.5	−0.5	252.50	36.01
95	10	12.5	22.5	0.25	0	−0.5	0.5	−0.5	260.71	42.25
96	9	12.5	22.5	0.25	−0.5	−0.5	0.5	−0.5	231.97	32.86

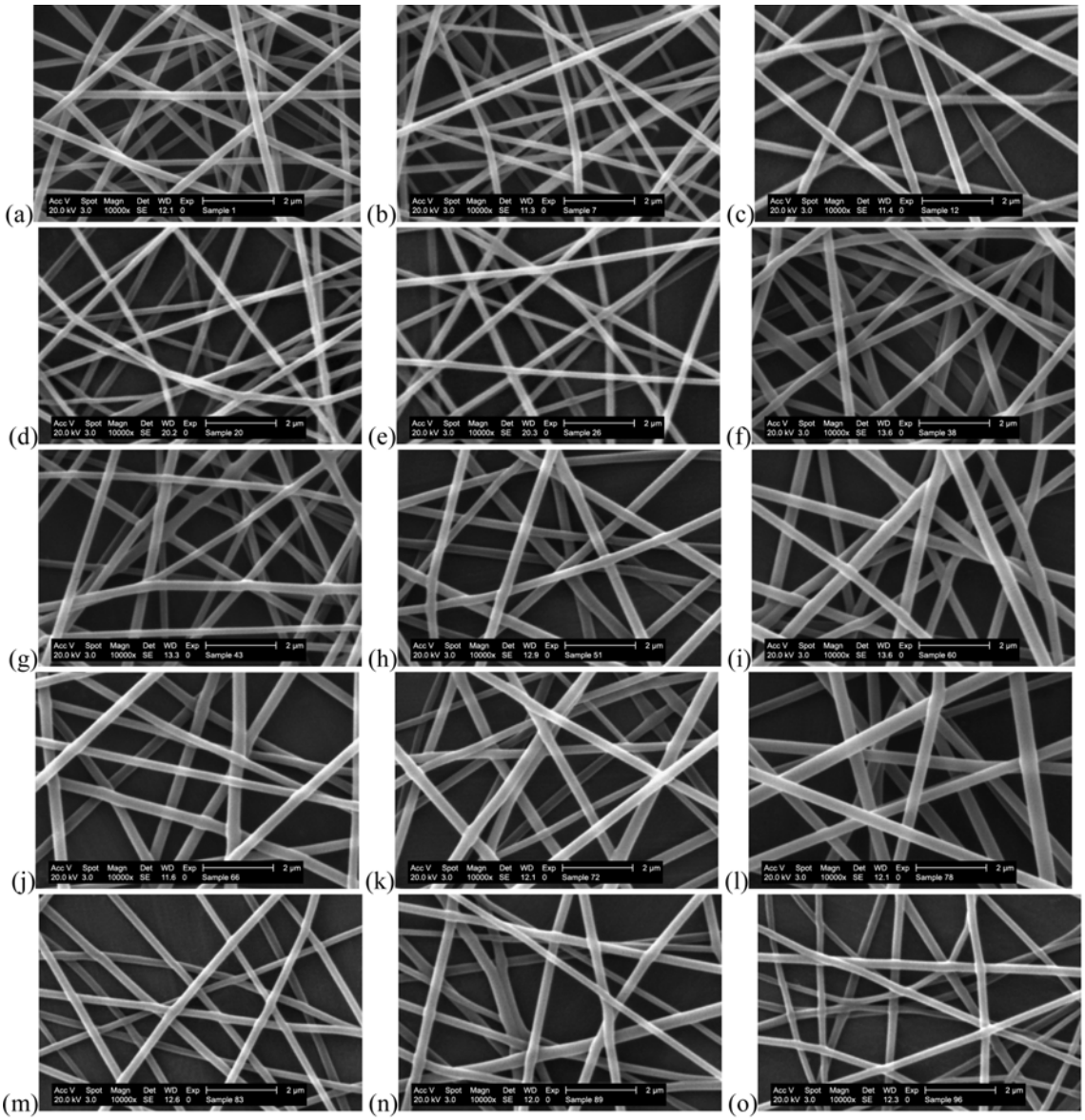

Fig. 5. SEM micrographs of typical PVA electrospun nanofiber mats: (a) C=8%, d=10 cm, V=15 kV, Q=0.2 ml/h, (b) C=8%, d=10 cm, V=25 kV, Q=0.2 ml/h, (c) C=8%, d=15 cm, V=15 kV, Q=0.4 ml/h, (d) C=8%, d=20 cm, V=15 kV, Q=0.3 ml/h, (e) C=8%, d=20 cm, V=25 kV, Q=0.3 ml/h, (f) C=10%, d=15 cm, V=15 kV, Q=0.3 ml/h, (g) C=10%, d=15 cm, V=25 kV, Q=0.2 ml/h, (h) C=10%, d=20 cm, V=20 kV, Q=0.4 ml/h, (i) C=12%, d=10 cm, V=20 kV, Q=0.4 ml/h, (j) C=12%, d=15 cm, V=15 kV, Q=0.4 ml/h, (k) C=12%, d=15 cm, V=25 kV, Q=0.4 ml/h, (l) C=12%, d=20 cm, V=20 kV, Q=0.4 ml/h, (m) C=10%, d=12.5 cm, V=15 kV, Q=0.3 ml/h, (n) C=10%, d=12.5 cm, V=22.5 kV, Q=0.3 ml/h, (o) C=9%, d=12.5 cm, V=22.5 kV, Q=0.25 ml/h.